

Geometrically Controlled 4-Point Interpolatory Schemes

Martin Marinov¹, Nira Dyn², and David Levin²

¹ Computer Graphics Group, RWTH Aachen, Germany
marinov@cs.rwth-aachen.de

² School of Mathematical Sciences, Tel-Aviv University, Israel
{niradyn|levin}@math.tau.ac.il

Summary. We present several non-linear 4-point interpolatory schemes, derived from the “classical” linear 4-point scheme. These new schemes have variable tension parameter instead of the fixed tension parameter in the linear 4-point scheme. The tension parameter is adapted locally according to the geometry of the control polygon within the 4-point stencil. This allows the schemes to remain local and in the same time to achieve two important shape-preserving properties - artifact elimination and convexity-preservation. The proposed schemes are robust and have special features such as “double-knot” edges corresponding to continuity without geometrical smoothness and inflection edges support for convexity-preservation. A convergence proof is given and experimental smoothness analysis is done in detail, which indicates that the limit curves are C^1 .

1 Introduction

1.1 An Overview of the 4-point Scheme

We explore the 4-point subdivision scheme [2] defined by the following mask:

$$p_{2i}^{k+1} = p_i^k, \quad (1)$$

$$p_{2i+1}^{k+1} = (p_i^k + p_{i+1}^k)(w + 1/2) - w(p_{i-1}^k + p_{i+2}^k), \quad (2)$$

where $\{p_i^k\}_i$ is a given control point sequence and w is a *tension parameter*. It is known that the 4-point scheme is C^1 for $0 < w < \frac{1}{8}$. The tension parameter plays a crucial rôle in the geometrically controlled schemes, so now we take a closer look at it. For the trivial value of $w = 0$ the 4-point scheme generates the piecewise linear interpolant to the initial control polygon. For the value $w = \frac{1}{16}$ the limit curve of the 4-point scheme has the best possible Hölder regularity $R_H = 2 - \varepsilon$, i.e., it is almost C^2 . Also, only for this value of w , the scheme reproduces polynomials of degree up to 3 [2]. For $0 < w < 1/16$,

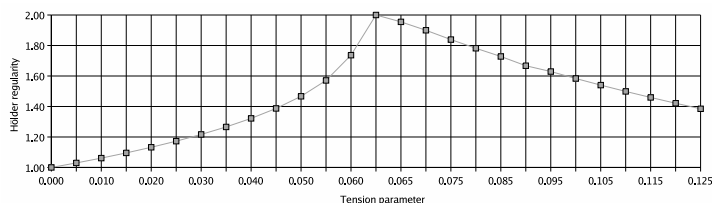


Fig. 1. Hölder regularity of the 4-point scheme for $w \in [0, \frac{1}{8}]$.

R_H is monotone in w , $1 \leq R_H < 2 - \varepsilon$ (Fig. 1). So for the value $w = \frac{1}{16}$ the 4-point scheme has the best regularity and approximation properties.

Fig. 2(upper left) demonstrates the visual effect when changing the tension parameter from 0 to $\frac{1}{16}$: for smaller w the generated curves are closer to the initial control polygon. With $w = \frac{1}{16}$, the smoothest curve is produced. However, $w = \frac{1}{16}$ may cause unpleasant problems as shown in Fig. 2(upper right). Lowering the tension parameter to $w = 0.01$ (Fig. 2(lower left)) solves these problems, but now the curve, which is still C^1 , is hardly recognisable visually from the initial control polygon. So we conclude that an appropriate choice of one tension parameter for an entire control polygon is not always possible.

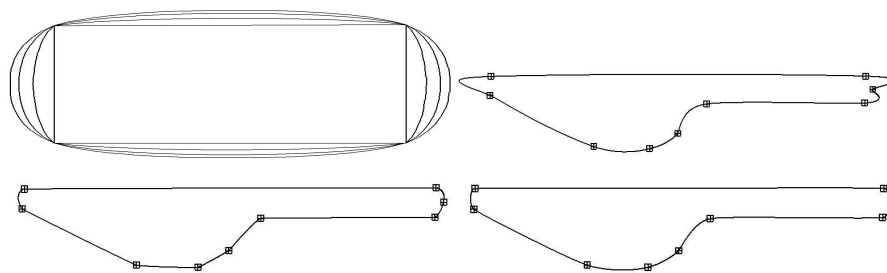


Fig. 2. (Upper left) the effect of w on the shape of the limit curve, (upper right) problems with the visual quality caused by $w = \frac{1}{16}$, (lower left) visually non-smooth curve caused by $w = 0.01$, (lower right) specific w_i^k for each edge of the control polygon alleviates the artifacts and keeps the visual appearance of the curve smooth enough.

1.2 Adaptive Tension Parameter

The idea of using different tension parameters for the edges of a given control polygon at each refinement step was initially investigated in [6]. While it was proved that the non-uniform 4-point scheme in the form

$$p_{2i}^{k+1} = p_i^k, \tag{3}$$

$$p_{e_i^k} = p_{2i+1}^{k+1} = (p_i^k + p_{i+1}^k)(w_i^k + 1/2) - w_i^k(p_{i-1}^k + p_{i+2}^k), \tag{4}$$

produces C^1 limit functions if w_i^k is always chosen in $[\varepsilon \dots \frac{1}{8} - \varepsilon]$ with $\varepsilon > 0$, one still needs to find a procedure for prescribing an appropriate w_i^k for every subdivision step. In this paper, we present several such procedures, where the choice of the tension parameter depends on the geometry of the control polygon. We call them *geometrically controlled* 4-point schemes or shortly *geometrically controlled* schemes.

For a given sequence of control points at refinement level k , $P^k = \{p_i^k\}_i$, where $p_i^k \in \mathbb{R}^2$ or $p_i^k \in \mathbb{R}^3$, we define $e_i^k = p_{i+1}^k - p_i^k$. The subdivision rule (2) is then expressed as

$$p_{e_i^k} = (p_i^k + p_{i+1}^k)(w + \frac{1}{2}) - w(p_{i-1}^k + p_{i+2}^k) = p_i^k + \frac{e_i^k}{2} + w(e_{i-1}^k - e_{i+1}^k). \tag{5}$$

This gives an interesting geometrical interpretation of the insertion rule of the 4-point scheme: the position of $p_{e_i^k}$ is actually a *displacement vector* d_i^k from the middle point of the edge e_i^k , which depends on the difference between the neighbouring edges, scaled by w . We extend its definition to the case of variable tension parameter:

$$d_i^k = w_i^k(e_{i-1}^k - e_{i+1}^k). \tag{6}$$

2 Displacement-safe Geometrically Controlled Schemes

2.1 Definition and Basic Properties

The first class of geometrically controlled schemes which we present here is aimed at solving problems in the shape of the limit curves such as those in the example in Fig. 2(upper right). There are two main questions which have to be answered in order to create such an *artifact-free* scheme:

1. How to detect possible locations in a given control polygon which create artifacts in the limit curve?
2. What subdivision rules to apply in such locations in order to avoid artifacts and at the same time to preserve the limit curve continuity and, if possible, its smoothness?

Our approach for selecting the tension parameter $w_i^k = \omega(i, k)$ tries to answer these two questions, by the composition of two functions $w_i^k = f(g(i, k))$:

1. a *characterising* function $g : I^k \rightarrow [0 \dots c]$. Here I^k is the set of all edge indices in a given refinement level k . $g(i, k)$ characterises the regularity of e_i^k in P^k .

2. a *selecting* function $f : [0 \dots c] \rightarrow [0 \dots W]$. $f(x)$ maps the range of $g(i, k)$ into the range of the available tension parameters.

We restrict our choice to functions which satisfy the following conditions:

1. $g(i, k)$ depends only on $p_{i-1}^k, p_i^k, p_{i+1}^k, p_{i+2}^k$, which ensures that our non-linear schemes have the same support as the original 4-point scheme.
2. $g(i, k)$ is invariant under similitudes.
3. $g(i, k) = 0 \Leftrightarrow |e_i^k| = 0$ and $f(x) = 0 \Leftrightarrow x = 0$, i.e., $w_i^k = 0 \Leftrightarrow |e_i^k| = 0$, i.e., we use the average operation for zero-length edges, thus creating corners. In the vicinity of such edges the limit curve is not G^1 anymore. We choose this behaviour for the following reasons:
 - a) To prevent the loops (see Fig. 8, row 3, column 1).
 - b) To mimic the behaviour of NURBS curves - while we keep the uniform parametrisation, we allow corners to be defined by repeated control points in the geometry.
4. $g(i, k) > 0 \Leftrightarrow |e_i^k| > 0$ and $0 < f(x) < W \Leftrightarrow x > 0$, where W is some predefined value for the tension parameter, corresponding to the regular edges. We usually take $W = \frac{1}{16}$.
5. $f(1) = W$. $g(i, k) = 1$ characterises the *regular* edges of P^k , i.e., areas where we can safely use subdivision rules which generate curves with maximum smoothness without creating artifacts.

We found out experimentally that the linear 4-point scheme produces visually-pleasing curves when the edges included in the insertion rule (5) are equidistant. Based on that observation we propose the following two possible combinations of characterising/selecting functions:

$$g(i, k) = \frac{3|e_i^k|}{|e_{i-1}^k| + |e_i^k| + |e_{i+1}^k|}, \quad f(x) = \begin{cases} Wx & , 0 \leq x \leq 1, \\ \frac{W(3-x)}{2} & , 1 < x \leq 3, \end{cases} \quad (7)$$

$$g(i, k) = \frac{3|e_i^k|}{|e_{i-1}^k| + |e_i^k| + |e_{i+1}^k|}, \quad f(x) = \begin{cases} Wx & , 0 \leq x \leq 1, \\ W & , 1 < x \leq 3. \end{cases} \quad (8)$$

We define $g(i, k) = 0$ if $|e_{i-1}^k| + |e_i^k| + |e_{i+1}^k| = 0$.

Furthermore, the geometrically controlled schemes should not introduce new corners during the subdivision process by multiplying consequent control points, i.e., creating zero-length edges. Therefore we introduce the notions:

Definition 1. A *geometrically controlled 4-point scheme* is safe if for every (i, k) , such that $|e_i^k| > 0$, the newly inserted control point $p_{e_i^k} = p_{2i+1}^{k+1}$ satisfies $p_{e_i^k} \neq p_{2i}^{k+1}$ and $p_{e_i^k} \neq p_{2i+2}^{k+1}$.

Definition 2. A *geometrically controlled 4-point scheme* is displacement-safe, if there exist $0 < C < \frac{1}{2}$, such that for every (i, k) such that $|e_i^k| \neq 0$, $|d_i^k| \leq C|e_i^k|$.

Lemma 1. *If a given geometrically controlled 4-point scheme is displacement-safe, then it is safe.*

Lemma 2. *If $0 < W < \frac{1}{8}$, then the geometrically controlled schemes defined by (7) or (8) are displacement-safe.*

Proof. Suppose that $g(i, k) \leq 1$. Then we have

$$|d_i^k| = \frac{3W |e_i^k|}{|e_{i-1}^k| + |e_i^k| + |e_{i+1}^k|} |e_{i-1}^k - e_{i+1}^k| < \frac{\frac{3}{8} |e_i^k| (|e_{i+1}^k| + |e_{i-1}^k|)}{|e_{i-1}^k| + |e_i^k| + |e_{i+1}^k|} \leq \frac{3}{8} |e_i^k|.$$

If $g(i, k) > 1$, then

$$\frac{3 |e_i^k|}{|e_{i-1}^k| + |e_i^k| + |e_{i+1}^k|} \geq 1 \Leftrightarrow 2 |e_i^k| \geq |e_{i-1}^k| + |e_{i+1}^k|,$$

Hence, if $g(i, k) > 1$, $|e_{i+1}^k - e_{i-1}^k| \leq |e_{i+1}^k| + |e_{i-1}^k| < 2 |e_i^k|$. Since $W > \frac{W(3-x)}{2}$ when $x > 1$ then

$$|d_i^k| \leq W |e_{i+1}^k - e_{i-1}^k| < 2W |e_i^k| < \frac{1}{4} |e_i^k|.$$

Corollary 1. *The two proposed geometrically controlled schemes are safe.*

An important consequence of the displacement-safe condition is that p_{2i+1}^{k+1} will be *close* to the subdivided edge e_i^k even if the neighbouring points p_{i-1}^k and p_{i+2}^k are very far away. A similar property is not true for the original 4-point scheme and our experiments show that it is the major reason for the appearance of artifacts in the generated limit curves. It also leads us to the idea of proposing a geometrical scheme based on the displacement-safe definition:

$$g(i, k) = \frac{C}{W} \frac{|e_i^k|}{|e_{i+1}^k - e_{i-1}^k|}, \quad f(x) = \min(Wx, W) \tag{9}$$

where $0 < C < \frac{1}{2}$, $0 < W < \frac{1}{8}$ and $g(i, k) = 0 \Leftrightarrow |e_{i+1}^k - e_{i-1}^k| = 0$. (9) performs on par with the two other proposed schemes in terms of visual quality, while having an additional global parameter C affecting its behaviour.

2.2 Convergence and Smoothness

We cite relevant results from [6].

Theorem 1. *If for every (i, k) , $w_i^k \in [0 : \frac{1}{8} - \varepsilon]$ for some $\varepsilon > 0$ then the non-uniform 4-point scheme (3), (4) produces C^0 limit functions. If for every (i, k) , $w_i^k \in [\varepsilon : \frac{1}{8} - \varepsilon]$ for some $\varepsilon > 0$ then the scheme (3), (4) generates C^1 limit functions.*

Corollary 2. *The proposed geometrically controlled displacement-safe schemes produce C^0 limit functions.*

Proof. By construction $w_i^k \in [0 : W]$, where $W \in [\varepsilon : \frac{1}{8} - \varepsilon]$ and we apply component-wise Theorem 1.

Remark 1. C^1 continuity of the limit curves of the displacement-safe schemes is not guaranteed since the tension parameters are not bounded away from zero. It can be achieved by the following modification. First we perform several unmodified subdivision steps; then, in every step, we select the new tension parameters so that they will not be smaller than those used in the previous step. Here are two possible strategies to achieve this:

$$w_{2i}^{k+1} = \max(\tilde{w}_{2i}^{k+1}, w_i^k), \quad w_{2i+1}^{k+1} = \max(\tilde{w}_{2i+1}^{k+1}, w_i^k) \quad \text{or}$$

$$w_{2i}^{k+1} = \max(\tilde{w}_{2i}^{k+1}, \min(w_i^k, w_{i-1}^k)), \quad w_{2i+1}^{k+1} = \max(\tilde{w}_{2i+1}^{k+1}, \min(w_i^k, w_{i+1}^k)),$$

where $\tilde{w}_{2i}^{k+1}, \tilde{w}_{2i+1}^{k+1}$ are computed as in the unmodified scheme. Since $w_i^k > 0$ away from the corner control points (which correspond to repeated vertices in the initial control polygon), and no new corner points are introduced during the subdivision, we can define $\varepsilon = \min_i \{w_i^K \mid w_i^K > 0\}$ for the last refinement step K used with the unmodified rules. Then in view of Theorem 1 this suffices for proving C^1 away from the predefined corners.

Although by applying these modified methods the displacement-safe condition is broken, the visual appearance of the limit curves is similar to the unmodified schemes limit curves, mainly because most of the artifacts are introduced in the first few steps. As in the unmodified schemes, the modified schemes do not increase the support of the 4-point scheme. The cost of using the modification is the additional memory required for keeping the values of the tension parameters used at the previous step.

3 Convexity-preserving Geometrically Controlled Scheme

An important shape-preserving property is convexity-preservation. A considerable amount of research related to subdivision schemes and convexity-preservation was conducted in [3, 4, 5]. The scheme proposed in [4] is the only one which works in the geometrical case, while the schemes investigated in [5] preserve convexity only in the functional case. The method presented in [3] chooses a global w depending on the initial convex functional data, such that the limit function of the 4-point scheme is convex.

Here we define a *geometrically controlled* scheme which preserves convexity in the geometrical case. The scheme handles correctly not only closed convex polygons (Fig. 3(left)), but also open convex polygons (Fig. 3(middle)) and other interesting cases (Fig. 3(right)).

We examine the 4-point scheme stencil for a given e_i^k and distinguish three configurations (Fig. 4):

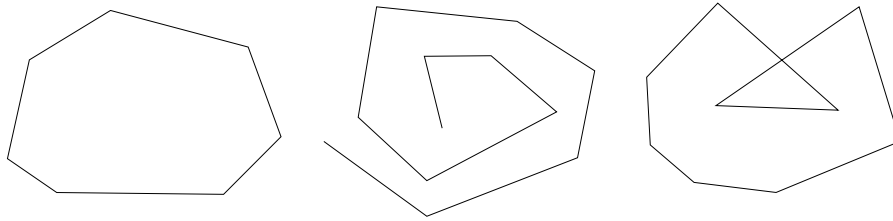


Fig. 3. Convex polygons – (left) closed, (middle) open, (right) self-intersecting.

Definition 3. $p_{i-1}^k, p_i^k, p_{i+1}^k, p_{i+2}^k$ form a convex stencil if p_{i-1}^k, p_{i+2}^k lie in a common half-plane with respect to the line defined by p_i^k, p_{i+1}^k . If at least one of p_{i-1}^k, p_{i+2}^k lies on the line through p_i^k, p_{i+1}^k , then the points form a straight stencil. Otherwise they form an inflection stencil.

Definition 4. e_i^k is a convex edge if $p_{i-1}^k, p_i^k, p_{i+1}^k, p_{i+2}^k$ form a convex stencil. It is a straight edge if the control points form a straight stencil. Otherwise it is an inflection edge.

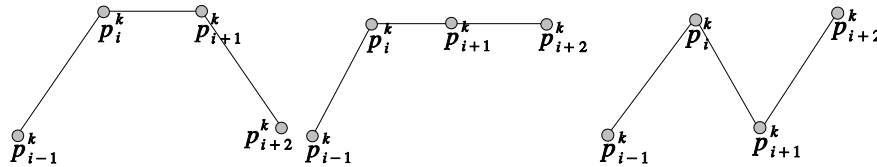


Fig. 4. Stencils – (left) convex, (middle) straight, (right) inflection.

Remark 2. Our definition for a convex stencil/edge is independent of the convexity of the edge with respect to the entire control polygon. So under *convex* we term both convex and concave stencils/edges in a given control polygon. However, in Sect. 4 we employ a special treatment to *inflection* edges and obtain co-convexity-preservation.

Definition 5. The polygon P^k is strictly convex if every e_i^k in P^k is convex.

Definition 6. The polygon P^k is convex if every e_i^k in P^k is either convex or straight.

Definition 7. A line t_i^k passing through p_i^k is a convex tangent if the points p_{i-1}^k, p_{i+1}^k lie in a common half-plane with respect to t_i^k . If p_{i-1}^k or p_{i+1}^k lies on t_i^k , it is a straight tangent. Otherwise t_i^k is an inflection tangent.

Suppose we have defined a convex tangent $\forall p_i^k \in P^k$. $\forall e_i^k$ we define the points $M_i^k = \frac{p_i^k + p_{i+1}^k}{2}$, $L_i^k = t_i^k \cap (M_i^k + \lambda_i^k \tilde{d}_i^k)$, $N_i^k = t_{i+1}^k \cap (M_i^k + \nu_i^k \tilde{d}_i^k)$, $\tilde{d}_i^k = e_{i-1}^k - e_{i+1}^k$, $\lambda_i^k, \nu_i^k \in \mathbb{R}$ (Fig. 5). We use the values λ_i^k, ν_i^k as bounds on w_i^k . In case $\lambda_i^k, \nu_i^k > 0$ we take $0 < w_i^k < \min(\lambda_i^k, \nu_i^k)$ in order to guarantee that if P^k is strictly convex, so is P^{k+1} . To see that this is necessary, assume that $w_i^k = \nu_i^k$ and $w_{i+1}^k = \lambda_{i+1}^k$. Then $p_{2i+1}^{k+1} = N_i^k$ and $p_{2i+3}^{k+1} = L_{i+1}^k$, and since $N_i^k \in t_{i+1}^k$ and $L_{i+1}^k \in t_{i+1}^k$, the points $p_{2i+1}^{k+1}, p_{2i+2}^{k+1} = p_{i+1}^k, p_{2i+3}^{k+1}$ lie on t_{i+1}^k and P^{k+1} fails to be strictly convex. So we define $\mu_i^k = C \cdot \min(\lambda_i^k, \nu_i^k)$, where $0 < C < 1$ is a user defined constant. We bound w_i^k in the range of values which guarantees convergence: $w_i^k = \min(W, \mu_i^k)$, where $0 < W < \frac{1}{8}$.

Remark 3. It is possible that $\lambda_i^k < 0$ or that $\nu_i^k < 0$. Negative bounds on w_i^k are ignored. We simply substitute $\lambda_i^k = \frac{W}{C}$ if $\lambda_i^k < 0$ and $\nu_i^k = \frac{W}{C}$ if $\nu_i^k < 0$.

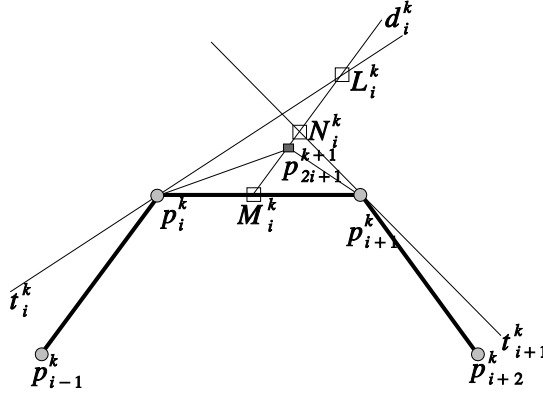


Fig. 5. Convexity-preserving scheme – inserting rule.

To prove that the resulting scheme is convexity-preserving and convergent we use the following notation, illustrated in Fig. 6:

- Every convex tangent t_i^k divides the plane in two half-planes: η_i^k and ξ_i^k such that $p_{i-1}^k, p_{i+1}^k \in \eta_i^k$.
- Every inflection tangent \hat{t}_i^k divides the plane into two half-planes: $\widehat{\eta}_i^k$ and $\widehat{\xi}_i^k$ such that $p_{i-1}^k \in \widehat{\eta}_i^k$ and $p_{i+1}^k \in \widehat{\xi}_i^k$.
- Every edge e_i^k defines a line l_i^k , which divides the plane in two half-planes: τ_i^k and σ_i^k .
- If e_i^k is convex, then $p_{i-1}^k, p_{i+2}^k \in \tau_i^k$.
- If e_i^k is inflection, then $p_{i-1}^k \in \tau_i^k$ and $p_{i+2}^k \in \sigma_i^k$.
- If e_i^k is straight, then either $p_{i+2}^k \in l_i^k$ and $p_{i-1}^k \in \tau_i^k$, or $p_{i-1}^k \in l_i^k$ and $p_{i+2}^k \in \sigma_i^k$.

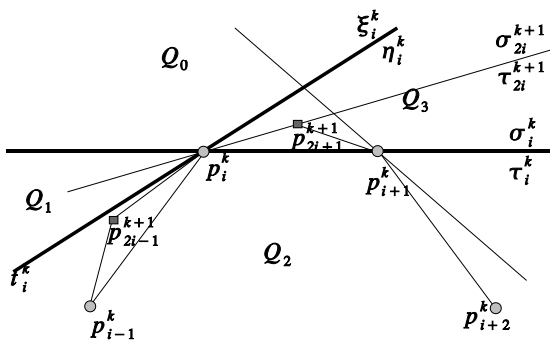


Fig. 6. Convexity-preserving scheme – illustration of the proof of Lemma 3.

Lemma 3. *If e_i^k and e_{i-1}^k belonging to an arbitrary P^k are convex, then e_{2i}^{k+1} and e_{2i-1}^{k+1} constructed by the convexity-preserving scheme are convex.*

Proof. Let us examine e_{2i}^{k+1} . The lines t_i^k and l_i^k , which cross at p_i^k , divide the plane into four quadrants $Q_0 = \xi_i^k \cap \sigma_i^k$, $Q_1 = \xi_i^k \cap \tau_i^k$, $Q_2 = \eta_i^k \cap \tau_i^k$ and $Q_3 = \eta_i^k \cap \sigma_i^k$ (Fig. 6). Since e_{i-1}^{k+1} and e_i^k are convex edges and t_i^k is a convex tangent then by construction $p_{2i+1}^{k+1} \in Q_3$ and $p_{2i-1}^{k+1} \in Q_2$. By definition, $p_{2i+2}^{k+1} = p_{i+1}^k \in Q_3 \cap Q_2$. Thus, the line l_{2i+1}^{k+1} containing e_{2i}^{k+1} is in the interior of the cone $Q_3 \cup Q_1$, and the points $p_{2i-1}^{k+1}, p_{2i+2}^{k+1}$ are in the same half-plane relative to e_{2i}^{k+1} . This proves that e_{2i}^{k+1} is convex. The proof of the convexity of e_{2i-1}^{k+1} is similar.

Remark 4. The requirement that e_{i-1}^k is convex is necessary for the convexity of e_{2i}^{k+1} , since in case e_{i-1}^k is an inflection edge and e_i^k is convex, it is possible to construct P^k such that e_{2i}^{k+1} is an inflection edge.

Remark 5. In the case that P^k is open, we treat the boundary edges $e_0^k, e_{N-1}^k \in P^k$ as convex, by adding “boundary points” p_{-1}^k, p_{N+1}^k such that e_1^{k+1} and e_{2N-2}^{k+1} are also convex. We do this is by taking $p_{-1}^k = p_0^k$ and $p_{N+1}^k = p_N^k$ and $t_0 \perp e_0$ and $t_N \perp e_{N-1}$. Any other choice of p_{-1}^k and p_{N+1}^k such that e_0^k and e_{N-1}^k are convex, generates convex boundary edges $e_1^{k+1}, e_{2N-2}^{k+1}$.

Corollary 3. *Given a strictly convex P^k , the refined control polygon P^{k+1} produced by the convexity-preserving scheme is also strictly convex.*

Proof. We apply Lemma 3 for every inner edge $e_i^{k+1} \in P^{k+1}$, and Remark 5 for the boundary edges.

The proposed scheme can handle correctly convex control polygons as well. If $p_{i-1}^k, p_i^k, p_{i+1}^k$ lie on the same line then a convex tangent t_i^k does not exist, and we take t_i^k to be a straight tangent. Application of the scheme with a straight

t_i^k obviously leads to $\mu_{i-1}^k = \mu_i^k = 0$, i.e., $w_{i-1}^k = w_i^k = 0$. Thus $e_{2i-2}^{k+1}, e_{2i-1}^{k+1}, e_{2i}^{k+1}, e_{2i+1}^{k+1}$ are straight. Furthermore if e_i^k is convex, but e_{i-1}^k is straight, then e_{2i}^{k+1} is also convex, since $p_{2i-1}^{k+1} \in e_{i-1}^k$ and the proof of Lemma 3 still applies. This proves the following claim:

Corollary 4. *Given a convex P^k , the refined control polygon P^{k+1} produced by the proposed scheme is also convex, so that for every convex $e_i^k \in P^k$ the edges $e_{2i}^{k+1}, e_{2i+1}^{k+1} \in P^{k+1}$ are convex and for every straight $e_i^k \in P^k$ the edges $e_{2i}^{k+1}, e_{2i+1}^{k+1} \in P^{k+1}$ are straight.*

Lemma 4. *Given an initial convex control polygon P^0 , the convexity-preserving scheme produces convex C^0 limit curve, which is a linear segment between the boundary points of each straight edge of P^0 and is a strictly convex curve between the boundary points of each strictly convex sub-polygon of P^0 .*

Proof. By construction $w_i^k \in [0 : W]$, where $W \in [\varepsilon : \frac{1}{8} - \varepsilon]$. Applying component-wise Theorem 1, we conclude that the scheme is convergent and that the limit curve is continuous.

Since all the edges between the boundary points of a straight edge in P^0 lie on that straight edge in every P^k , the limit curve is a line segment between these two boundary points. To see that the limit curve between the boundary points of a strictly convex sub-polygon of P^0 is strictly convex, assume that part of such a segment of the limit curve is a line segment s . Then for k large enough there are three points $p_{i-1}^k, p_i^k, p_{i+1}^k$ on s . This contradicts Corollary 4, since all edges in P^k between the boundary points of a convex edge in P^0 are convex and the strictly convex sub-polygon consists only of convex edges.

We propose the following ways to approximate the tangents t_i^k :

1. $t_i^k = p_{i+1}^k - p_{i-1}^k$
2. $t_i^k \perp b_i^k$, where b_i^k is the bisector of the angle defined by $p_{i-1}^k, p_i^k, p_{i+1}^k$
3. t_i^k is the tangent at p_i^k of the the circle passing through $p_{i-1}^k, p_i^k, p_{i+1}^k$

The first method is the simplest and most natural. The tangent coincides with the tangent of the quadratic function passing through $p_{i-1}^k, p_i^k, p_{i+1}^k$, it is easy and fast to compute and it gives the best results in visual quality. Certainly other choices are also possible.

4 Co-convex Geometrically Controlled Scheme

While convexity-preservation is a very useful property it is still not enough to handle a lot of “real world” situations. Artists and engineers which employ CAD systems often desire to have the freedom to define curves which consist of convex and concave parts, joined smoothly. Here we present an extension of the scheme defined in Sect. 3 that produces curves which preserve convexity

and concavity according to the convexity/concavity of the edges of the initial control polygon. We call it the *co-convex* geometrically controlled 4-point scheme.

As we mentioned in Remark 4, in case e_{i-1}^k is an inflection edge, it is not enough that e_i^k is convex for e_{2i}^{k+1} to be convex. To guarantee that e_{2i}^{k+1} is convex when e_i^k is convex, we have to ensure that $p_{2i-1}^{k+1} \in \tau_{2i}^{k+1}$. We define additional inflection tangents $\widehat{t}_i^k, \widehat{t}_{i+1}^k$ for the boundary points p_i^k, p_{i+1}^k of an inflection edge e_i^k and compute $\widehat{L}_i^k = \widehat{t}_i^k \cap (M_i^k + \lambda_i^k \widehat{d}_i^k), \widehat{N}_i^k = \widehat{t}_{i+1}^k \cap (M_i^k + \nu_i^k \widehat{d}_i^k), \lambda_i^k, \nu_i^k \in \mathbb{R}$ (Fig. 7(left)). We replace the negative values among $\lambda_i^k, \nu_i^k, \widehat{\lambda}_i^k, \widehat{\nu}_i^k$ with $\frac{W}{C}$ and select w_i^k for e_i^k as:

$$\mu_i^k = C \cdot \min \left(\lambda_i^k, \nu_i^k, \widehat{\lambda}_i^k, \widehat{\nu}_i^k \right), \quad w_i^k = \min(W, \mu_i^k), \quad 0 < W < \frac{1}{8}$$

We define the inflection tangents \widehat{t}_i^k as the bisector of the angle defined by $p_{i-1}^k, p_i^k, p_{i+1}^k$. Any other line dividing this angle can also be used. For $k > 0$ we do not employ convexity-preserving rules when subdividing edges which are descendants of the inflection edges in the refinement hierarchy of P^0 - we use the original 4-point scheme for them (Fig. 7(right)). To see why, examine the following 4-point stencil: $p_{i-1}^0 = (0, -1), p_i^0 = (0, 0), p_{i+1}^0 = (1, 0), p_{i+2}^0 = (1, 1)$. Regardless of the used tangents the inserted point is $p_{2i+1}^1 = (0, 0.5)$. Therefore the configuration $p_{2i}^1, p_{2i+1}^1, p_{2i+2}^1$ is straight and if we apply the convexity-preserving rule, it will lead to a line segment on the limit curve between p_i^0 and p_{i+1}^0 . Still this is probably not the intention of the designer, who can add an additional point on the edge e_i^0 in order to create a straight segment in the curve.

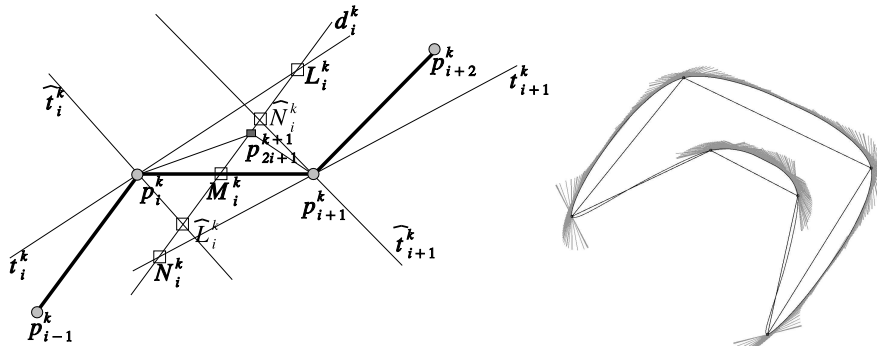


Fig. 7. Co-convex scheme – (left) insertion rule for an inflection edge, (right) co-convex limit curve with the computed convex tangents. Note the segments corresponding to the inflection edges where the linear 4-point scheme is used.

Lemma 5. *If the edge $e_i^k \in P^k$ is convex, then the edges e_{2i}^{k+1} and e_{2i+1}^{k+1} constructed by the proposed co-convex scheme are convex.*

Proof. Let us examine e_{2i}^{k+1} . In case e_{i-1}^k is convex, we apply Lemma 3. If e_{i-1}^k is an inflection edge, then $p_i^k \in \widehat{\xi}_i^k$ with respect to the tangent t_i^k and by construction $p_{2i-1}^{k+1} \in (\eta_i^k \cap \widehat{\eta}_i^k) \subset Q_2$, which implies the convexity of e_{2i}^{k+1} . The proof for e_{2i+1}^{k+1} is analogous.

Remark 6. If the subdivided edge e_i^k defines a corner, i.e., $|e_i^k| = 0$, then similar to the schemes defined in Sect. 2 we prevent loops by using $w_i^k = 0$. If $|e_i^k| = 0$, but $|e_{i-1}^k| > 0$ we treat e_{i-1}^k as convex edge and define the tangent $t_i^k \perp e_{i-1}$. By symmetry if $|e_{i+1}^k| > 0$, we define the tangent $t_{i+1}^k \perp e_{i+1}$.

Finally we are able to define a robust co-convex scheme with the following properties:

Lemma 6. *Given an arbitrary control polygon P^0 the proposed co-convex scheme produces a C^0 limit curve with the following properties: (a) For every convex sub-polygon of P^0 the corresponding curve segment is strictly convex. (b) For every straight edge e_i^0 the corresponding curve segment is a line segment. (c) All inflection points on the curve are contained in segments of the curve corresponding to inflection edges in P^0 .*

Remark 7. A corner point or a control point p_i^0 in P^0 joining two consecutive straight edges e_{i-1}^0 and e_i^0 can also be inflection points in the limit curve.

Remark 8. The convexity-preserving and co-convex schemes which we propose can be easily applied to 3D control points. Given a tangent line, we define a tangent plane $T_i^k = \{P : P = \lambda_0 t_i^k + \lambda_1 (e_{i-1}^k \times e_i^k) + p_i^k\}$. Then all intersections are performed using the tangent plane. If $e_{i-1}^k \times e_i^k = \emptyset$, then either $e_i^k = \emptyset$ or $e_{i-1}^k = \emptyset$, or e_i^k and e_{i-1}^k are on the same line. The first two cases are corner cases and we can define T_i^k to be perpendicular to the non-zero edge. The third one is a straight configuration and every tangent plane passing through the line defined by e_i^k can be used.

Remark 9. One could also combine the co-convex scheme with a displacement-safe scheme in order to get rid of artifacts. This is done easily by taking the minimum of the tension parameters determined by the two schemes. The resulting tension parameter satisfies both conditions and thus the limit curve is artifact-free and co-convex.

5 Experimental Analysis of Smoothness and Examples

For non-linear schemes the conventional tools for checking smoothness are not applicable. An experimental method for analyzing these schemes is employed

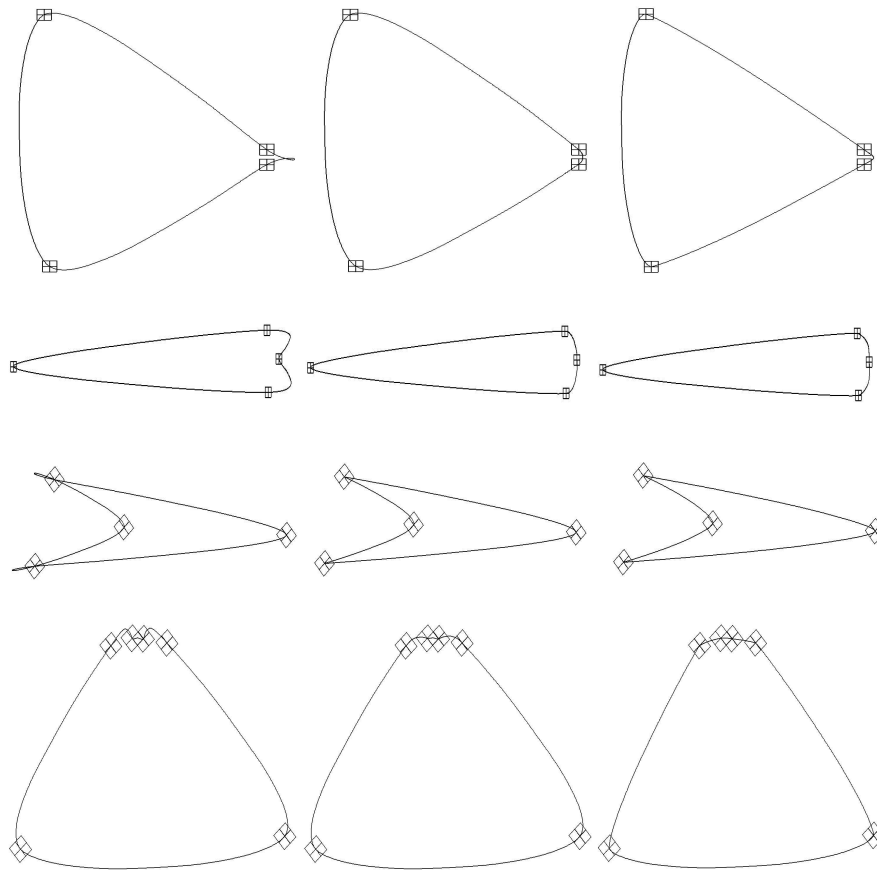


Fig. 8. Examples: left column – the original 4-point scheme with $w = 1/16$, middle column – the displacement-safe scheme (9) with $C = 0.2$, right column – the convexity-preserving scheme with $C = 0.9$.

in [1, 5] by checking numerically the Hölder regularity of several computed limit curves. Since the parametrization we use is uniform, we can employ the algorithm proposed in [5], which is related to the following definitions:

Definition 8. An l times differentiable function $f : \Omega \subset R \rightarrow R$ is said to have Hölder regularity $R_H = l + \alpha$, if there exist $C < \infty$ such that:

$$\left| \frac{\partial^l f(x_1)}{\partial x_1^l} - \frac{\partial^l f(x_2)}{\partial x_2^l} \right| \leq C |x_1 - x_2|^\alpha, \forall x_1, x_2 \in \Omega.$$

Definition 9. An interpolatory subdivision scheme is said to have Hölder regularity $R_H = l + \alpha_l$, if there exist $C < \infty$ and $h > 0$ such that:

$$\lim_{k \rightarrow \infty} l!2^{kl} |(\Delta^l f^k)_{i+1} - (\Delta^l f^k)_i| \leq C(2^{-k}h)^{\alpha_l}$$

where $(\Delta f^k)_i = f_{i+1}^k - f_i^k$ and Δ^l is defined recursively as $\Delta \Delta^l f = \Delta^{l+1} f$.

We define $\rho_l^k = l!2^{kl} \max_i |(\Delta^l f^k)_{i+1} - (\Delta^l f^k)_i|$ and under the assumption that $\rho_l^k \approx C(2^{-k}h)^{\alpha_l}$, one can define the contraction factor λ_l and compute an estimate of α_l :

$$\lambda_l := \frac{\rho_l^{k+1}}{\rho_l^k} \approx \frac{C(2^{-(k+1)}h)^{\alpha_l}}{C(2^{-k}h)^{\alpha_l}} = 2^{-\alpha_l}, \quad \alpha_l := -\log_2 \left(\frac{\rho_l^{k+1}}{\rho_l^k} \right).$$

Computing α_l makes sense only if $\alpha_j \approx 1$ for $j = 0, 1, \dots, l - 1$. The proposed method is verified by applying it to schemes for which R_H has been determined analytically - for example the 4-point scheme with $w = \frac{1}{16}$ is proved to have $R_H = 2 - \varepsilon$, and the above method obtains numerically the values $\alpha_1 \approx 1$ and $\alpha_2 \approx 0$. Our implementation checks α_l of the geometrically controlled schemes component-wise, i.e., for $f_i = x_i$ we compute α_l^x , for $f_i = y_i$ we compute α_l^y , and for $f_i = z_i$ we compute α_l^z . α_l then is defined as $\alpha_l = \min(\alpha_l^x, \alpha_l^y, \alpha_l^z)$.

Since R_H of the original 4-point scheme depends on the tension parameter, not surprisingly the geometrically controlled schemes have different R_H depending on the initial geometry. We tested the proposed schemes on the examples given in the paper and we also applied the schemes (7), (8) and the co-convex scheme on about 220K randomly generated control polygons (Fig. 9). All of the curves generated by the schemes (7), (8) after 18 subdivision steps were C^1 , i.e., $\alpha_0 \approx 1$ and $\alpha_1 > 0$, while only 0.019% of the curves generated by the co-convex scheme were not C^1 . This leads us to the conclusion that the proposed displacement-safe schemes are most probably C^1 , and the co-convex scheme is also C^1 away from corners and straight edges. It is clear also, that the co-convex scheme sacrifices regularity in order to achieve convexity-preservation in some cases (Fig. 9).

Acknowledgement

This work was supported by the European Union research project “Multiresolution in Geometric Modelling (MINGLE)” under grant HPRN-CT-1999-00117.

References

1. Aspert, N., Ebrahimi, T., Vandergheynst, P.: Non-linear subdivision using local spherical coordinates. *Computer Aided Geometric Design*, 20, 165–187 (2003).
2. Dyn, N., Gregory, J., Levin., D.: A 4-point interpolatory subdivision scheme for curve design. *Computer Aided Geometric Design*, 4, 257–268 (1987).

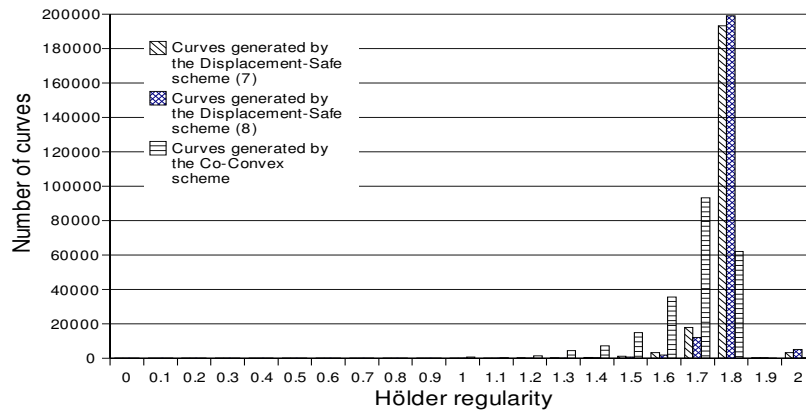


Fig. 9. Experimental Hölder regularity of the limit curves generated by the displacement-safe schemes (7), (8) and the co-convex scheme with $C = 0.9$ applied to 219436 randomly generated control polygons, $W = \frac{1}{16}$. The scheme (9) was not included in the experiment, since its parameter C is a tradeoff between analytical smoothness and visual quality and therefore can not be determined automatically.

3. Dyn, N., Kuijt, F., Levin, D., van Damme, R. M. J.: Convexity preservation of the four-point interpolatory subdivision scheme. *Computer Aided Geometric Design*, 16, 789–792 (1999).
4. Dyn, N., Levin, D., Liu, D.: Interpolatory convexity-preserving subdivision schemes for curves and surfaces. *Computer Aided Geometric Design*, 24, 211–216 (1992).
5. Kuijt, F.: Convexity Preserving Interpolation - Stationary Nonlinear Subdivision and Splines. PhD thesis, University of Twente, Faculty of Mathematical Sciences, (1998).
6. Levin, D.: Using Laurent polynomial representation for the analysis of the non-uniform binary subdivision schemes. *Advances in Computational Mathematics*, 11, 41–54 (1999).